J. Fluid Mech. (1995), *vol.* 286, *pp.* 103–116

Free-surface flow generated by a small submerged circular cylinder starting from rest

By PEDER A. TYVAND[1] AND TOUVIA MILOH[2]

[1] Department of Agricultural Engineering, Agricultural University of Norway, 1432 Ås, Norway

[2] Department of Fluid Mechanics and Heat Transfer, Tel Aviv University, Ramat Aviv, Tel Aviv 69 978, Israel

(Received 4 January 1994 and in revised form 27 September 1994)

The impulsively starting motion of a small circular cylinder submerged horizontally below a free surface is studied analytically using a small-time expansion. The cylinder is considered small if the ratio between its radius and initial submergence depth is much smaller than one. The surface elevation is calculated up to third order. The hydrodynamic force on the small cylinder is also discussed. Certain inconsistencies in our small-cylinder approximation (assuming locally uniform flow around the cylinder) are found in the force prediction. The present work is an accompanying paper to Tyvand & Miloh (1995), where the same problem is studied for arbitrary radius versus submergence depth.

1. Introduction

Havelock (1949) performed the first study of a submerged circular cylinder starting from rest near a free surface. He investigated the full time evolution of the free surface, based on linear theory. Tuck (1965) carried this type of analysis into the nonlinear regime.

The present work complements the earlier analytical approach to Havelock's problem: we investigate the short-time evolution of the full nonlinear initial/boundary value problem, applying a small-time expansion (Peregrine 1972). In a paper written in parallel with the present one (Tyvand & Miloh 1995, hereafter referred to as TM) we develop an exact theory for arbitrary cylinder size, and solve the problem in terms of Fourier expansions in bipolar coordinates. In the present paper, simple formulae for the small-cylinder limit are derived, based on the hypothesis of uniform local flow around the cylinder. The small-cylinder limit is the leading order of an expansion with respect to a parameter assumed much smaller than one: the ratio between the cylinder radius and its initial submergence depth.

The full initial/boundary value problem for an impulsively started submerged cylinder has been studied numerically by Haussling & Coleman (1979), Telste (1987), Greenhow (1988, 1993) and Terent'ev (1991). Greenhow & Lin (1983) have investigated the present problem experimentally for the case of vertical motion.

2. Mathematical problem

We consider a solid circular cylinder of radius $\Re$ submerged in an inviscid incompressible fluid of infinite depth. At negative times ($t < 0$) everything is at rest, and the cylinder centre is located at a distance D below the free surface of the fluid. Cartesian coordinates x and y are introduced. The x-axis lies at the undisturbed free

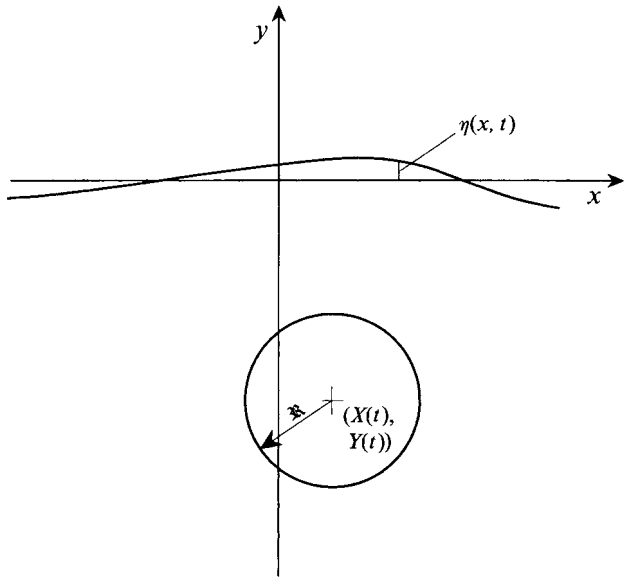

FIGURE 1. Definition sketch of the moving cylinder and free surface.

surface, see figure 1. The y-axis is directed upwards. The gravitational acceleration is denoted by g. The surface elevation is denoted by $\eta(x,t)$. We introduce a unit velocity W, which is the constant forced velocity of the cylinder. The unit of length is the initial submergence depth D. The important dimensionless parameter in the present formulation is the Froude number defined by

$$Fr = \frac{W}{(gD)^{1/2}}. \tag{2.1}$$

We also introduce units of dimensionless time D/W and pressure ρW^2, where ρ is the fluid density. The dimensionless cylinder radius is chosen as

$$\epsilon = \Re/D. \tag{2.2}$$

The forced motion starts impulsively from rest at time zero. The flow is governed by Laplace's equation

$$\nabla^2 \Phi = 0, \tag{2.3}$$

where $\Phi(x,y,t)$ is the dimensionless velocity potential. The dimensionless boundary conditions are

$$|\nabla \Phi| \to 0, \quad x^2 + y^2 \to \infty, \tag{2.4}$$

$$\frac{\partial \eta}{\partial t} + \frac{\partial \Phi}{\partial x}\frac{\partial \eta}{\partial x} = \frac{\partial \Phi}{\partial y}, \quad y = \eta(x,t), \tag{2.5}$$

$$\frac{\partial \Phi}{\partial t} + \tfrac{1}{2}|\nabla \Phi|^2 + Fr^{-2}\eta = 0, \quad y = \eta(x,t). \tag{2.6}$$

The position of the cylinder centre is written as

$$\boldsymbol{R}(t) = X(t)\boldsymbol{i} + Y(t)\boldsymbol{j}, \tag{2.7}$$

where $\boldsymbol{i}$ and $\boldsymbol{j}$ are unit vectors in the x- and y-directions, respectively. Our initial conditions are chosen as (TM)

$$\eta(x,0) = 0, \tag{2.8}$$

$$\Phi(x,0,0) = 0. \tag{2.9}$$

We choose ρW^2 as a reference pressure. The units of dimensionless mass, force and momentum (per length along the cylinder) are given by (ρD^2), $(\rho D W^2)$ and $\rho D^2 W)$, respectively (see TM).

3. The small-time expansion

Our nonlinear initial/boundary value problem is solved analytically by employing a small-time expansion (e.g. Peregrine 1972; Greenhow & Lin 1983). We then postulate (see TM)

$$(\Phi, \eta, \boldsymbol{R}) = (0, 0, \boldsymbol{R}_0) + H(t)[(\Phi_0, 0, 0) + t(\Phi_1, \eta_1, \boldsymbol{R}_1) + t^2(\Phi_2, \eta_2, \boldsymbol{R}_2) + \ldots] \quad (-\infty < t < \infty). \tag{3.1}$$

Here the Heaviside unit step function has been introduced:

$$H(t) = 0, \quad t \leqslant 0 \quad \text{and} \quad H(t) = 1, \quad t > 0. \tag{3.2}$$

In (3.1) the instantaneous position vector of the cylinder centre is prescribed by its forced motion:

$$\boldsymbol{R}_n = \boldsymbol{i} X_n + \boldsymbol{j} Y_n \quad (n = 0, 1, 2, \ldots), \tag{3.3}$$

where we have already defined

$$(X_0, Y_0) = (0, -1). \tag{3.4}$$

The governing equations and free-surface boundary conditions are the same as in our preceding paper (TM, (3.5)–(3.13)). But for the boundary conditions at the cylinder contour, our present small-cylinder analysis will be independent of TM.

By the principle of superposition we may split the potential into two contributions at each order, i.e.

$$\Phi_n = \phi_n + \psi_n \quad (n = 0, 1, 2, \ldots). \tag{3.5}$$

The first term (ϕ_n) is generated by the inhomogeneous condition at the free surface with zero normal derivative at the cylinder contour. The second term (ψ_n) is generated by the inhomogeneous boundary condition at the cylinder contour, with a homogeneous condition at the free surface. In the present small-cylinder limit ψ_n will be represented by a moving-dipole potential.

The small-time expansion for the hydrodynamic force is

$$\boldsymbol{F} = \boldsymbol{F}_{-1}\,\delta(t) + (\boldsymbol{F}_0 + \boldsymbol{F}_1 t + \boldsymbol{F}_2 t^2 + \ldots) H(t). \tag{3.6}$$

Here $\delta(t)$ is Dirac's delta function, which is the derivative of the Heaviside unit step function $H(t)$. As in TM we omit the constant hydrostatic force in this series expansion, since, unlike the other contributions, it is not turned on at time zero.

4. On the dipole potential and the surface elevation

When the ratio of cylinder radius to initial submergence depth (ϵ) is small, there is a leading dipole contribution to the zeroth-order potential (see e.g. Batchelor 1967, p. 424). For a cylinder in unbounded fluid with a general motion prescribed by (2.7), the exact potential for the induced fluid flow is

$$\Phi = -\epsilon^2 \dot{\boldsymbol{R}} \cdot (\boldsymbol{r} - \boldsymbol{R})\, |\boldsymbol{r} - \boldsymbol{R}|^{-2}. \tag{4.1}$$

The non-expanded version of the moving-dipole potential is then given by

$$\psi = \epsilon^2 \dot{X}\left(\frac{-x+X}{(x-X)^2+(y-Y)^2} + \frac{x-X}{(x-X)^2+(y+Y)^2}\right) - \epsilon^2 \dot{Y}\left(\frac{y-Y}{(x-X)^2+(y-Y)^2} + \frac{y+Y}{(x-X)^2+(y+Y)^2}\right) + O(\epsilon^4). \tag{4.2}$$

			(*a*) (i) $\epsilon = 0.1$, $N = 10$			
$\|x\|$	0	0.25	0.5	1.0	1.5	3.0
$\eta_1 \times 10^2$	2.000	1.659	0.956	0.002	−0.237	−0.159
dipole	2	1.661	0.96	0	−0.237	−0.16
			(ii) $\epsilon = 0.3$, $N = 20$			
$\|x\|$	0	0.25	0.5	1.0	1.5	3.0
$\eta_1 \times 10$	1.799	1.481	0.834	0.020	−0.217	−0.139
dipole	1.8	1.495	0.864	0	−0.213	−0.144
			(*b*) (i) $\epsilon = 0.1$, $N = 10$			
x	0	0.25	0.5	1.0	1.5	3.0
$\eta_1 \times 10^2$	0	0.888	1.281	0.997	0.566	0.119
dipole	0	0.886	1.28	1	0.568	0.12
			(ii) $\epsilon = 0.3$, $N = 20$			
x	0	0.25	0.5	1.0	1.5	3.0
$\eta_1 \times 10$	0	0.811	1.156	0.878	0.490	0.102
dipole	0	0.797	1.152	0.9	0.511	0.108

TABLE 1. First-order surface elevation. Exact Fourier series solution (4.6) is truncated after N terms. Comparisons are made with the surface elevation in the small-cylinder limit (dipole solution (4.5)). (*a*) Vertical motion: $\alpha = \frac{1}{2}\pi$, (*b*) horizontal motion: $\alpha = 0$.

This potential can be expanded by introducing the power series $X(t)$ and $Y(t)$ for the forced motion. Equation (4.2) is derived from (4.1) by adding appropriate image potentials in order to satisfy the homogeneous boundary condition $\psi = 0$ at $y = 0$. Equation (4.2) has been proven to be consistent with the higher-order boundary conditions at the cylinder contour in our preceding paper (TM, (3.19)–(3.22)).

All higher-order elevations due to the forced motion of the cylinder are included in the following expression:

$$\frac{\partial \psi}{\partial y}(x,0) = -4\epsilon^2 \dot{X} \frac{(x-X)\,Y}{((x-X)^2+Y^2)^2} + 2\epsilon^2 \dot{Y}\left(\frac{2Y^2}{((x-X)^2+Y^2)^2} - \frac{1}{(x-X)^2+Y^2}\right) + O(\epsilon^4). \quad (4.3)$$

The zeroth-order small-cylinder solution is constructed by putting $t = 0$ in the moving-dipole potential (4.2).

Our following analysis will be restricted to the realm of the small-time expansion. We introduce the angle α between the velocity vector and the x-axis (measured in the counter-clockwise direction):

$$X_1 = \cos\alpha, \quad Y_1 = \sin\alpha. \quad (4.4)$$

The first-order elevation generated by the dipole potential (4.2) is

$$\eta_1 = 4\epsilon^2 X_1 \frac{x}{(x^2+1)^2} + 2\epsilon^2 Y_1 \frac{1-x^2}{(x^2+1)^2}. \quad (4.5)$$

The first-order elevation is written here as a sum of two terms: first the contribution due to the horizontal motion, which is antisymmetric about the y-axis and has a maximum at $x = 0.5774$ $(= 1/\sqrt{3})$; secondly, the contribution due to the vertical motion, which changes sign at $x = 1$.

The first-order surface elevation usually differs from the exact solution by less than

0.3 % when $\epsilon < 0.1$. See tables 1(*a*) and 1(*b*), where comparisons with the exact theory (TM) are made. When $\epsilon = 0.3$ the dipole approximation typically leads to deviations of order 3 % from the exact solution. The dipole solution begins to fail when ϵ exceeds 0.5, and when $\epsilon > 0.8$ it makes no sense at all. These conclusions are about the same for higher-order solutions, although there is a tendency for greater deviations from the small-cylinder limit solution. The exact first-order elevation is derived in TM (§5) in terms of bipolar coordinates. We rewrite it here explicitly in Cartesian coordinates:

$$\eta_1 = \frac{4(1-\epsilon^2)}{x^2+1-\epsilon^2} \sum_{n=1}^{\infty} (-1)^{n+1} n \exp(-n \operatorname{arcsech} \epsilon) \times \operatorname{sech}(n \operatorname{arcsech} \epsilon) \sin\left[2n \arctan \frac{x}{(1-\epsilon^2)^{1/2}} + \alpha\right]. \quad (4.6)$$

We will now study the first-order potential in the small-cylinder limit. It is given by the inhomogeneous boundary condition (TM, (3.9))

$$\phi_1(x,0) = -\tfrac{1}{2}\eta_1^2 = -\frac{\epsilon^4}{(x^2+1)^4}[a_1 x^2 + a_2(1-x^2)^2 + a_3 x(1-x^2)], \quad (4.7a)$$

where

$$a_1 = 8\cos^2\alpha, \quad a_2 = 2\sin^2\alpha, \quad a_3 = 4\sin 2\alpha. \quad (4.7b)$$

Instead of solving the higher-order problems by residue calculus, we introduce two classes of harmonic functions defined at the boundary:

$$f_m(x,0) = (x^2+1)^{-m} \quad (m = 1,2,\ldots), \quad (4.8)$$

$$g_m(x,0) = x(x^2+1)^{-m} \quad (m = 1,2,\ldots). \quad (4.9)$$

In the Appendix these functions are derived for $m < 5$.

The first-order potential (4.7) can be written as a sum of these functions:

$$\phi_1(x,0) = \epsilon^4[a_1(-f_3+f_4) + a_2(-f_2+4f_3-4f_4) + a_3(g_3-2g_4)]_{y=0}. \quad (4.10)$$

After applying the relationships in the Appendix, we end up with the small-cylinder limit of the second-order elevation due to the convective acceleration at the free surface:

$$\frac{1}{2}\frac{\partial\phi_1}{\partial y}(x,0) = \epsilon^4[\tfrac{1}{4}f_1 + f_2 - 2f_3 + 2\cos 2\alpha(5f_3 - 20f_4 + 16f_5) + 2\sin 2\alpha(-g_3 + 12g_4 - 16g_5)]_{y=0}. \quad (4.11)$$

The term in the last parentheses represents the leading-order nonlinear hydrodynamic interaction between the horizontal and vertical motion. At $x = 0$ (4.11) reduces to

$$\frac{1}{2}\frac{\partial\phi_1}{\partial y}(0,0) = \epsilon^4(2\cos 2\alpha - \tfrac{3}{4}). \quad (4.12)$$

The leading nonlinear hydrodynamic effect at the free surface reduces the height of the surface mound in the case of vertical motion. When the cylinder is moved horizontally, one effect of the convective acceleration is to increase the size of the surface trough and reduce the size of the surface crest. The second-order surface elevation due to the nonlinear effects at the free surface has an amplitude about twice as large for vertical motion as for horizontal motion.

By expanding (4.3) we find the contribution to the second-order elevation due to the moving dipole:

$$\frac{1}{2}\frac{\partial\psi_1}{\partial y}(x,0) = \epsilon^2\left[\frac{4X_2 x + 2Y_2(1-x^2)}{(x^2+1)^2} + 2\frac{(3x^2-1)\cos 2\alpha + x(3-x^2)\sin\alpha}{(x^2+1)^3}\right]. \quad (4.13)$$

			(*a*) (i) $\epsilon = 0.1$			
$\|x\|$	0	0.25	0.5	1.0	1.5	3.0
$\eta_2 \times 10^2$	1.963	1.336	0.259	−0.495	−0.333	−0.051
asymptotic	1.973	1.343	0.262	−0.496	−0.334	−0.052
			(ii) $\epsilon = 0.3$			
$\|x\|$	0	0.25	0.5	1.0	1.5	3.0
$\eta_2 \times 10$	1.501	1.069	0.254	−0.408	−0.282	−0.041
asymptotic	1.577	1.128	0.279	−0.420	−0.294	−0.047
			(*b*) (i) $\epsilon = 0.1$			
$\|x\|$	0	0.25	0.5	1.0	1.5	3.0
$\eta_2 \times 10^2$	−1.983	−1.352	−0.265	0.499	0.337	0.052
asymptotic	−1.988	−1.354	−0.266	0.499	0.336	0.052
			(ii) $\epsilon = 0.3$			
$\|x\|$	0	0.25	0.5	1.0	1.5	3.0
$\eta_2 \times 10$	−1.657	−1.190	−0.302	0.440	0.315	0.051
asymptotic	−1.699	−1.216	−0.308	0.440	0.312	0.050
			(*c*) (i) $\epsilon = 0.1$			
x	−3.0	−1.5	−1.0	−0.5	−0.25	
$\eta_2 \times 10^2$	−0.037	−0.063	−0.499	−1.398	−1.212	
asymptotic	−0.036	−0.065	−0.501	−1.401	−1.214	
x	0	0.25	0.5	1.0	1.5	3.0
$\eta_2 \times 10^2$	−0.010	1.197	1.392	0.503	0.067	−0.036
asymptotic	−0.008	1.203	1.398	0.504	0.068	−0.036
			(ii) $\epsilon = 0.3$			
x	−3.0	−1.5	−1.0	−0.5	−0.25	
$\eta_2 \times 10$	0.038	−0.045	−0.439	−1.188	−1.001	
asymptotic	0.035	−0.058	−0.460	−1.214	−1.015	
x	0	0.25	0.5	1.0	1.5	3.0
$\eta_2 \times 10$	−0.078	0.880	1.264	0.470	0.068	−0.029
asymptotic	−0.061	0.927	1.184	0.480	0.077	−0.030

TABLE 2. Second-order surface elevation: $\eta_2(x) = \frac{1}{2}(\partial \Phi_1 \partial y)_{y=0}$. Exact Fourier series solution (4.15)+(4.16) is truncated after 10 terms in both n and m. Comparisons are made with our small-cylinder asymptotic solution (4.11)+(4.13). (*a*) Vertical motion: $\alpha = \frac{1}{2}\pi$; (*b*) horizontal motion $\alpha = 0$; (*c*) oblique motion $\alpha = \frac{1}{4}\pi$.

Here we have introduced the angle α defined by (4.4). The total second-order elevation is the sum of the two terms (4.11) and (4.13). Equation (4.13) represents the leading-order 'geometric nonlinearity', due to the cylinder centre being displaced from its initial position as soon as a finite time has passed since the start. For small cylinders it dominates over the hydrodynamic nonlinearity at the free surface (4.11), because it is of two orders lower in ϵ.

Let us discuss the case of constant upward vertical velocity ($\alpha = \frac{1}{2}\pi$), where (4.13) simplifies to

$$\frac{1}{2}\frac{\partial \psi_1}{\partial y}(x, 0) = 2\epsilon^2 \frac{(1-3x^2)}{(x^2+1)^3}. \tag{4.14}$$

We note that geometric nonlinearity increases the size of the surface mound, and it displaces the point of zero surface elevation below $|x| = 1$. Both these effects are opposite to the leading-order effects of hydrodynamic nonlinearity, i.e. convective acceleration at the free surface. The first-order amplitude is known to be larger the

closer a given cylinder is to the free surface. Thus it is clear that the surface amplitude above the cylinder must be increased due to geometric nonlinearity, since this effect accounts for the basic fact that the cylinder is displaced towards the free surface: the first-order elevation alone pretends that the cylinder contour is at rest, 'pumping' a normal flow into the lower half and out through the upper half of the fixed contour.

In the case of a constant horizontal velocity ($\alpha = 0$), the second-order elevation due to the moving dipole is minus that for vertical motion (4.14). In this case the geometric nonlinearity reduces the depth of the surface trough for $x < 0$ and increases the height of the surface crest for $x > 0$. This is opposite to the leading-order effects of hydrodynamic nonlinearity at the free surface. The best way to interpret this case is to note that geometric nonlinearity displaces the total crest/trough pattern to the right. It also tends to make the surface trough wider and more shallow, while the crest becomes narrower and steeper.

In tables 2(*a*)–2(*c*) the sum of (4.11) and (4.13) is compared with the exact solution (for constant speed) derived in TM (§7): the exact second-order elevation is the sum of the following two contributions, rewritten in Cartesian coordinates:

$$\begin{aligned}\frac{1}{2}\frac{\partial \phi_1}{\partial y}(x,0) = {} & \frac{(1-\epsilon^2)^{1/2}}{16(x^2+1-\epsilon^2)} \sum_{n=1}^{\infty}\sum_{m=1}^{\infty} (-1)^{n+m} nm \exp\left[-(n+m)\,\mathrm{arcsech}\,\epsilon\right] \\ & \times \mathrm{sech}\,(n\,\mathrm{arcsech}\,\epsilon)\,\mathrm{sech}\,(m\,\mathrm{arcsech}\,\epsilon) \\ & \times \sum_{k=-2}^{2} (24-9k^2+k^4) \sum_{q=-1}^{1} q(n+qm+k) \\ & \times \cos\left[2(n+qm+k)\arctan\frac{x}{(1-\epsilon^2)^{1/2}} + (q+1)\,\alpha\right] \\ & \times \tanh\left[(n+qm+k)\,\mathrm{arcsech}\,\epsilon\right], \end{aligned} \tag{4.15}$$

$$\begin{aligned}\frac{1}{2}\frac{\partial \psi_1}{\partial y}(x,0) = {} & -\sin\alpha \frac{(1-\epsilon^2)^{1/2}}{x^2+1-\epsilon^2} \\ & \times \sum_{n=1}^{\infty} (-1)^n n \exp\left(-n\,\mathrm{arcsech}\,\epsilon\right) \mathrm{sech}\,(n\,\mathrm{arcsech}\,\epsilon) \\ & \times \left\{(n-1)\sin\left[2(n-1)\arctan\frac{x}{(1-\epsilon^2)^{1/2}} + \alpha\right]\tanh\left[(n-1)\,\mathrm{arcsech}\,\epsilon\right]\right. \\ & + 2n\sin\left[2n\arctan\frac{x}{(1-\epsilon^2)^{1/2}} + \alpha\right]\tanh\left(n\,\mathrm{arcsech}\,\epsilon\right) \\ & \left. + (n+1)\sin\left[2(n+1)\arctan\frac{x}{(1-\epsilon^2)^{1/2}} + \alpha\right]\tanh\left[(n+1)\,\mathrm{arcsech}\,\epsilon\right]\right\} \\ & - \frac{2\cos\alpha}{x^2+(1-\epsilon^2)^{1/2}} \sum_{n=1}^{\infty} (-1)^n n \exp\left(-n\,\mathrm{arcsech}\,\epsilon\right) \mathrm{sech}\,(n\,\mathrm{arcsech}\,\epsilon) \\ & \times \left[\sin\left(2\arctan\frac{x}{(1-\epsilon^2)^{1/2}}\right)\sin\left(2n\arctan\frac{x}{(1-\epsilon^2)^{1/2}} + \alpha\right)\right. \\ & \left. - 2n\frac{1-\epsilon^2}{x^2+1-\epsilon^2}\cos\left(2n\arctan\frac{x}{(1-\epsilon^2)^{1/2}} + \alpha\right)\right]. \end{aligned} \tag{4.16}$$

We have performed separate comparisons for hydrodynamic nonlinearity ((4.15) *vs.* (4.11)) and geometric nonlinearity ((4.16) *vs.* (4.13)). These comparisons are similar, so we present only their sums in table 2.

The leading-order gravitational effect (superscript Fr) in the small-cylinder limit is found by combining (TM (3.10)) and (4.5):

$$\phi_2^{(Fr)}(x,0) = \frac{\epsilon^2}{Fr^2}[-2X_1 g_2 + Y_1(f_1 - 2f_2)]_{y=0}. \tag{4.17}$$

In the Appendix these three harmonic functions g_1, f_1 and f_2 are derived.

The relationships derived in the Appendix also give the gravitational effect on the third-order elevation:

$$\eta_3^{(Fr)}(x) = \epsilon^2 Fr^{-2}\left[X_1 \frac{2g_2 - 8g_3}{3} + Y_1 \frac{6f_2 - 8f_3}{3}\right]_{y=0}. \tag{4.18}$$

Here we have applied the kinematic condition (TM (3.14)). We note the expected result (for vertical motion) that the leading-order gravitational effect gives negative surface elevation near $x = 0$, corresponding to outward radiation of gravity waves. We do not compare the small-cylinder expression (4.18) with the exact formula in TM, because such a comparison is implicit in table 2: the exact expression is proportional to the first of the two infinite series occurring in (4.16); the one with the factor $(\sin\alpha)$.

5. On the hydrodynamic force

Below we will see that our present small-cylinder expansion provides a fully consistent approximation for the force only in the lowest order (the 'order minus one' with the singular δ-function term). The reason that it may fail at higher orders is that the assumption of locally uniform flow around the cylinder is too crude for some of the force contributions, no matter how small the cylinder is. However, our small-cylinder expansion is consistent for the surface elevation to any order, as demonstrated in tables 1 and 2.

The dipole solution itself disregards all feedback from the free surface on the local zeroth-order flow around the cylinder. However, there is one feedback effect that influences the leading-order modification of the flow surrounding the cylinder, which is given by (regarded as locally uniform)

$$-\boldsymbol{R}_1(1 - \tfrac{1}{2}\epsilon^2).$$

The correction term $-\frac{1}{2}\epsilon^2$ for the relative flow is composed of two equal contributions: (i) due to the flow generated by the image cylinder (its infinite-fluid dipole moment); (ii) the other due to the image-induced (feedback) modification of the local dipole moment of the cylinder, and thereby of its self-induced flow. The inclusion of this feedback correction is necessary to satisfy the boundary condition at the cylinder contour. We generalize this result to also apply for an arbitrary cylinder position:

$$\boldsymbol{U} = \left(-1 + \frac{\epsilon^2}{2Y^2}\right)\frac{\mathrm{d}\boldsymbol{R}}{\mathrm{d}t}. \tag{5.1}$$

The physical meaning of this expression is as follows: $\boldsymbol{U}$ represents the instantaneous surrounding flow field experienced by a small cylinder, in the infinite Froude number (vanishing gravity) limit, provided no significant nonlinear free-surface effects have

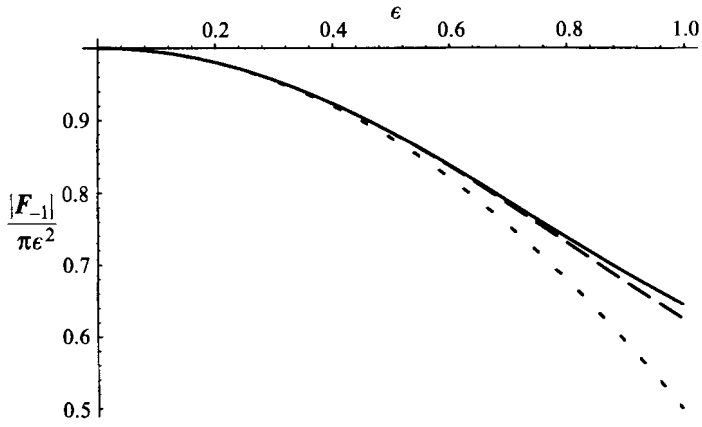

FIGURE 2. Impulse force on the cylinder, divided by infinite-fluid added mass, given as a function of the cylinder radius. Solid curve: exact formula (5.6). Dashed curve: three-term asymptotic expansion (5.5). Dotted curve: two-term asymptotic expansion (5.4).

been accumulated since the motion was started impulsively. The time derivative of (5.1) reads

$$\frac{\mathrm{d}\boldsymbol{U}}{\mathrm{d}t} = \left(-1+\frac{\epsilon^2}{2Y^2}\right)\frac{\mathrm{d}^2\boldsymbol{R}}{\mathrm{d}t^2} - \frac{\epsilon^2}{Y^3}\frac{\mathrm{d}Y}{\mathrm{d}t}\frac{\mathrm{d}\boldsymbol{R}}{\mathrm{d}t}. \tag{5.2}$$

To obtain a force estimate, we have to multiply this acceleration with the mass of the fluid displaced by the cylinder. This force is the hydrodynamic force expected to be experienced by a deeply submerged cylinder in very rapid motion (the infinite Froude-number limit). However, it will be shown below that this small-cylinder theory is never fully consistent with respect to the force. Therefore we will refrain from discussing (5.2) further in its general form. Such a discussion has been given by Greenhow (1988, equation 1), for the case of vertical motion. But (5.2) is in principle incorrect as a basis for calculating the force, except during the impulsive start itself. However, it leads to only small errors when the motion is vertical.

Let us expand in powers of time the added-mass force due to the time derivative of the relative flow surrounding the cylinder, according to (5.2):

$$\boldsymbol{F}^{(dipole)}/(\pi\epsilon^2) = -(\boldsymbol{R}_1\,\delta(t)+2\boldsymbol{R}_2)(1-\tfrac{1}{2}\epsilon^2)+H(t)\,(\epsilon^2 Y_1\,\boldsymbol{R}_1+O(t)). \tag{5.3}$$

The superscript *dipole* is meant to indicate that this force only takes into account the dipole solution (modified by a zero-potential free-surface condition), not the nonlinear interaction with the free surface.

Using (5.3) we derive the following dipole approximation:

$$\boldsymbol{F}_{-1}/(\pi\epsilon^2) = -(1-\tfrac{1}{2}\epsilon^2)\,\boldsymbol{R}_1, \tag{5.4}$$

which is asymptotically valid for $\epsilon \to 0$, and can also be easily deduced from the analysis of Milne-Thomson (1968). However, we carry the asymptotic expansion (5.4) one step further by extending our argument preceding (5.2). Considering the infinite-fluid dipole moment at the cylinder location as unity, it will induce a unit image dipole. This image dipole again induces an upward surrounding flow of $\frac{1}{4}\epsilon^2$ around the cylinder. However, this gives a feedback reduction of the unit dipole moment to $(1-\frac{1}{4}\epsilon^2)$. This again reduces the image dipole moment to $(1-\frac{1}{4}\epsilon^2)$, so its upward flow generated around the cylinder is reduced to $\frac{1}{4}\epsilon^2-\frac{1}{16}\epsilon^4$. This gives a second feedback modification of the unit dipole moment to $(1-\frac{1}{4}\epsilon^2+\frac{1}{16}\epsilon^4)$, which represents the self-induced relative flow.

Adding the (downward) self-induced and the (upward) image-induced relative flows we find that the total (downward) surrounding flow experienced by the cylinder is $(1-\frac{1}{2}\epsilon^2+\frac{1}{8}\epsilon^4)$. In terms of added-mass force this can be written

$$|\boldsymbol{F}_{-1}|/(\pi\epsilon^2) = 1-\tfrac{1}{2}\epsilon^2+\tfrac{1}{8}\epsilon^4. \tag{5.5}$$

For all $\epsilon < 0.5$ the graphical representation of (5.5) follows very closely the exact curve (TM, §6), which can be expressed by

$$\boldsymbol{F}_{-1} = -4\pi\boldsymbol{R}_1(1-\epsilon^2)\sum_{n=1}^{\infty} n\exp(-2n\,\mathrm{arcsech}\,\epsilon)\tanh(n\,\mathrm{arcsech}\,\epsilon). \tag{5.6}$$

In figure 2 this exact formula is displayed, together with the three-term, (5.5), and two-term, (5.4), asymptotic expansions for small ϵ. Equivalent exact formulae for the impulsive force (5.6) have earlier been derived by Venkatesan (1985) and Greenhow & Li (1987).

From the expressions in the Appendix we find the first-order velocities at the cylinder location induced by the leading-order convective acceleration at the free surface:

$$\frac{\partial\phi_1}{\partial x}(0,-1) = -\tfrac{1}{8}\epsilon^4\sin 2\alpha, \tag{5.7a}$$

$$\frac{\partial\phi_1}{\partial y}(0,-1) = \tfrac{1}{8}\epsilon^4(\cos 2\alpha-2). \tag{5.7b}$$

These expressions gives the leading-order nonlinear free-surface effects on the induced flow at the cylinder location. Equation (5.7*a*) shows that the horizontal flow component arises due to nonlinear interaction between the zeroth-order horizontal and vertical flows. This induced horizontal flow has its maximum when the initial velocity vector makes an angle of $\frac{1}{4}\pi$ with each coordinate axis. This is no such interaction effect on the vertical flow. Equation (5.7*b*) shows that nonlinear free-surface effects always give a downward flow. The magnitude of the downward flow has its minimum when the motion is horizontal, and reaches its maximum (three times that minimum) when the motion is vertical. The magnitude of the downward first-order flow is at least twice that of the horizontal first-order flow.

A basic qualitative question is whether the early nonlinear free-surface effects will increase or reduce the hydrodynamic force. Our formulae (5.7) show that the leading-order nonlinear effects will increase the magnitude of the surrounding flow velocity experienced by the cylinder. This tends to increase the force components.

We will now investigate the zeroth-order force, which is a time-independent force on the cylinder. This is the dominating force on the cylinder just after the cylinder has been forced impulsively into motion. The total zeroth-order force for constant speed ($X_2 = Y_2 = 0$) can be written (see TM, §8):

$$\boldsymbol{F}_0 = \boldsymbol{F}_0^{(dyn)} + \boldsymbol{F}_0^{(free)} + \boldsymbol{F}_0^{(geom)}. \tag{5.8}$$

The zeroth-order force is the sum of three different effects: (i) the dynamic-pressure effect (superscript *dyn*) due to the zeroth-order tangential flow along the cylinder contour; (ii) the first-order flow due to the leading-order nonlinear effects of the convective acceleration at the free surface (superscript *free*); (iii) the geometric nonlinearity in the first-order flow (superscript *geom*), accounting for the fact that the cylinder centre is being displaced out from its initial position at any finite time since the start.

The first term in (5.8) will have asymptotic limit zero, according to our hypothesis of uniform local flow around the cylinder, since the dynamic pressures balance each other on each side of the cylinder. But the exact theory of TM shows that this force is of order ϵ^4 when the cylinder radius ϵ is small.

From (5.7) we derive the following expression which may only be valid asymptotically in the small-cylinder limit:

$$\boldsymbol{F}_0^{(free)}/(\pi\epsilon^2) \sim \tfrac{1}{4}\epsilon^4[-\boldsymbol{i}\sin 2\alpha + \boldsymbol{j}(\cos 2\alpha - 2)]. \tag{5.9}$$

In TM §8 we confirm that this is indeed the correct small-cylinder limit for the second term in (5.8). However, it is of smaller order of magnitude than the first term in (5.8). Thus we cannot find a consistent small-cylinder limit for the total force with our present type of small-cylinder approximation.

With our hypothesis of uniform local flow around the cylinder, (5.3) gives the present small-cylinder approximation for the third term in (5.8):

$$\boldsymbol{F}_0^{(geom)}/(\pi\epsilon^2) \sim \epsilon^2 \boldsymbol{R}_1 \sin\alpha = \tfrac{1}{2}\epsilon^2[\boldsymbol{i}\sin 2\alpha + \boldsymbol{j}(1-\cos 2\alpha)]. \tag{5.10}$$

There is an inherent inconsistency in the prediction (5.10) itself. To understand this, we follow TM (Appendix B) and split the zeroth-order force due to the geometric nonlinearity into two contributions:

$$\boldsymbol{F}_0^{(geom)} = \tilde{\boldsymbol{F}}_0^{(geom)} + \overset{\star}{\boldsymbol{F}}_0^{(geom)}. \tag{5.11}$$

In our context, the first of these force contributions arises because the cylinder convects its surrounding dipole field (including its image) into a new location. This term alone is in full agreement with our small-cylinder prediction (5.10). The second contribution in (5.11) accounts for the fact that the cylinder penetrates a finite distance into the initial flow field (that continues to operate, as it is steadily building up the first-order elevation). This 'penetration' effect is lost completely in our small-cylinder approximation, and this is the cause of the inconsistency. TM shows that this second term in (5.11) is of the same order of magnitude as the first term (except that it is zero for purely vertical motion). Thus our force prediction (5.10) is an inconsistent small-cylinder limit.

The leading gravitational effects on the hydrodynamic force are specified by linear theory. So the principle of super-position is valid for the gravitational surface elevation and force when the cylinder performs an oblique motion. The gravitational flow generated at the cylinder location is

$$\frac{\partial \phi_2^{(Fr)}}{\partial x}(0,-1) = -\frac{\epsilon^2\cos\alpha}{4Fr^2}, \tag{5.12a}$$

$$\frac{\partial \phi_2^{(Fr)}}{\partial y}(0,-1) = -\frac{\epsilon^2\sin\alpha}{4Fr^2}. \tag{5.12b}$$

Thus the leading-order gravitational effect gives a positive contribution to the magnitude of the relative flow surrounding the cylinder. This contribution grows as a quadratic function of time. It gives a gravitational hydrodynamic force that grows linearly with time, because a basic force-generating mechanism in the small-cylinder limit is the time derivative of the relative flow, (5.2). This gravitational force contribution points in the direction opposite to the forced initial motion of the cylinder. It is given by

$$\boldsymbol{F}_1^{(Fr)}/(\pi\epsilon^2) = -(\epsilon^2/Fr^2)\,\boldsymbol{R}_1. \tag{5.13}$$

The second-order gravitational flow (5.12) increases the effective surrounding flow experienced by the cylinder. This causes a feedback increment of the dipole moment of the cylinder (necessary to satisfy the boundary condition at its contour), which again increases the effective surrounding flow by the same amount as that given by (5.12). Because of time differentiation, the flow amplitude occurring on the right-hand side in (5.13) becomes four times that of (5.12).

6. Summary

A small-time expansion has been performed for the unsteady nonlinear free-surface flow generated by the forced motion of a circular cylinder being impulsively started from rest. The surface elevation and the hydrodynamic force are calculated in the three lowest orders of the expansion, according to our small-cylinder limit where the flow is taken to be locally uniform around the cylinder. In our tables 1 and 2 comparisons are made with the exact surface elevation (TM), showing good agreement when the dimensionless cylinder radius is 0.3 or smaller.

Both the initial added-momentum force and the leading gravitational force are vectors pointing in a direction opposite to the motion of the cylinder. Thus reversing the direction of motion means reversing these forces. As a contrast, the steady (zeroth-order) force is unchanged when the direction of motion is reversed. The steady hydrodynamic force is proportional to the square of the velocity, and is purely vertical both for horizontal and vertical motion. A horizontal steady force component arises only in the case of oblique motion. This force component arises from nonlinear interactions between the zeroth-order flows due to horizontal and vertical motion of the cylinder.

The present work is carried out in Cartesian coordinates, but has evolved in parallel with the exact theory (TM) given in bipolar coordinates. The present small-cylinder limit is useful in checking the more complicated exact formulae of TM. Our present approximation for the surface elevation is fully consistent, and all comparisons between the exact theory and the small-cylinder limit are given only in the present paper and omitted in TM. For more details on a similar comparison for the force components, we refer to TM where relevant graphs are displayed.

Our small-cylinder hypothesis of uniform flow surrounding the cylinder is inconsistent with respect to the zeroth-order force. Nevertheless it works for the singular impulsive force, as well as for the first-order gravitational force. These inconsistencies help us to clarify the different physical effects contributing to the zeroth-order force. In TM we identify two distinct effects that are completely lost in our small-cylinder approximation: (i) the dynamic-pressure force, and (ii) the finite penetration into the initial flow field. These are the roots of the inconsistencies.

E. E. Leirgul is thanked for drawing figure 1. Dr E. Plahte is thanked for his help with computing the tables.

Appendix. On linear combinations of image multipoles

For our study of higher-order elevations in the small-cylinder limit it is useful to introduce the two following classes of harmonic functions defined at the boundary $y = 0$:

$$f_m(x,0) = (x^2+1)^{-m} \quad (m = 1,2,\ldots), \tag{A 1}$$

$$g_m(x,0) = x(x^2+1)^{-m} \quad (m = 1,2,\ldots). \tag{A 2}$$

A conventional way to determine these functions is by residue calculus based on Poisson's integral formula. But we can find the same information from successive differentiations of the point source potential χ located in the image point $(x, y) = (0, 1)$:

$$\chi = \tfrac{1}{2}\log(x^2+(y-1)^2). \tag{A 3}$$

These functions are linear combinations of multipoles with their centre in the image point (0, 1). Immediately we have

$$f_1(x,y) = -\frac{\partial\chi}{\partial y} = \frac{1-y}{x^2+(y-1)^2}, \tag{A 4}$$

$$g_1(x,y) = \frac{\partial\chi}{\partial x} = \frac{x}{x^2+(y-1)^2}. \tag{A 5}$$

We differentiate each of these functions four successive times with respect to y and get the relationships

$$\partial f_1/\partial y = -f_1 + 2f_2, \tag{A 6}$$

$$f_2 = (2-5y-x^2y+4y^2-y^3)/[2(x^2+(y-1)^2)^2], \tag{A 7}$$

$$\partial f_2/\partial y = -\tfrac{1}{2}f_1 - 2f_2 + 4f_3, \tag{A 8}$$

$$f_3 = \frac{8-33y-12x^2y-3x^4y+54y^2+18x^2y^2-44y^3-6x^2y^3+18y^4-3y^5}{8(x^2+(y-1)^2)^3}, \tag{A 9}$$

$$\partial f_3/\partial y = -\tfrac{3}{8}f_1 - \tfrac{3}{4}f_2 - 3f_3 + 6f_4, \tag{A 10}$$

$$f_4 = (16-93y-47x^2y-23x^4y-5x^6y+232y^2+144x^2y^2+40x^4y^2-323y^3-162x^2y^3 \\ -15x^4y^3+272y^4+80x^2y^4-139y^5-15x^2y^5+40y^6-5y^7)/[16(x^2+(y-1)^2)^4], \tag{A 11}$$

$$\partial f_4/\partial y = -\tfrac{5}{16}f_1 - \tfrac{1}{2}f_2 - f_3 - 4f_4 + 8f_5, \tag{A 12}$$

$$\partial g_1/\partial y = 2g_2 = 2x(1-y)/(x^2+(y-1)^2)^2, \tag{A 13}$$

$$\partial g_2/\partial y = -g_2 + 4g_3, \tag{A 14}$$

$$g_3 = x(4-9y-x^2y+6y^2-y^3)/[4(x^2+(y-1)^2)^3], \tag{A 15}$$

$$\partial g_3/\partial y = -\tfrac{1}{4}g_2 - 2g_3 + 6g_4, \tag{A 16}$$

$$g_4 = \frac{x(8-29y-6x^2y-x^4y+40y^2+8x^2y^2-26y^3-2x^2y^3+8y^4-y^5)}{8(x^2+(y-1)^2)^4}, \tag{A 17}$$

$$\partial g_4/\partial y = -\tfrac{1}{8}g_2 - \tfrac{1}{2}g_3 - 3g_4 + 8g_5. \tag{A 18}$$

REFERENCES

BATCHELOR, G. K. 1967 *An Introduction to Fluid Dynamics*. Cambridge University Press.

GREENHOW, M. 1988 Water-entry and -exit of a horizontal circular cylinder. *Appl. Ocean Res.* **10**, 191–198.

GREENHOW, M. 1993 A complex variable method for the floating-body boundary-value problem. *J. Comput. Appl. Maths* **46**, 115–128.

GREENHOW, M. & LI, Y. 1987 Added masses for circular cylinders near or penetrating fluid boundaries – review, extension and application to water-entry, -exit and slamming. *Ocean Engng* **14**, 325–348.

GREENHOW, M. & LIN, W.-M. 1983 Nonlinear free surface effects: experiments and theory. *Rep.* 83–19. MIT, Dept. of Ocean Engineering.

HAUSSLING, H. J. & COLEMAN, R. M. 1979 Nonlinear water waves generated by an accelerated circular cylinder. *J. Fluid Mech.* **92**, 767–781.

HAVELOCK, T. H. 1949 The wave resistance of a cylinder started from rest. *Q. J. Mech. Appl. Maths* **2**, 325–334.

MILNE-THOMSON, L. M. 1968 *Theoretical Hydrodynamics*. MacMillan.

PEREGRINE, D. H. 1972 Flow due to a vertical plate moving in a channel. Unpublished note.

TELSTE, J. G. 1987 Inviscid flow about a cylinder rising to a free surface. *J. Fluid Mech.* **182**, 149–168.

TERENT'EV, A. G. 1991 Nonstationary motion of bodies in a fluid. *Proc. Steklov Inst. Maths* **186**, 211–221.

TUCK, E. O. 1965 The effect of nonlinearity on flow past a submerged cylinder. *J. Fluid Mech.* **22**, 401–414.

TYVAND, P. A. & MILOH, T. 1995 Free-surface flow due to impulsive motion of a submerged circular cylinder. *J. Fluid Mech.* **286**, 67–101 (referred to herein as TM).

VENKATESAN, S. K. 1985 Added mass of two cylinders. *J. Ship Res.* **29**, 234–240.